UNITED STATES
DEPARTMENT OF THE INTERIOR
GEOLOGICAL SURVEY

GEOPHYSICAL INVESTIGATIONS OF THE UMM AR RUMMF COPPER PROSPECT, AL QUNFUDHAH QUADRANGLE, KINGDOM OF SAUDI ARABIA

BY

Hamdy S. Sadek and H. Richard Blank

U.S. Geological Survey
Open-File Report 83-298

Prepared for:

Ministry of Petroleum and Mineral Resources
Deputy Ministry for Mineral Resources
Jiddah, Kingdom of Saudi Arabia
1403 AH 1982 AD

1983

CONTENTS

ILLUSTRATIONS
[Plates are in back pocket]

Page

TABLES

GEOPHYSICAL INVESTIGATIONS OF THE UMM AR RUMMF COPPER PROSPECT, AL QUNFUDHAH QUADRANGLE, KINGDOM OF SAUDI ARABIA

by

Hamdy S. Sadek and H. Richard Blank

ABSTRACT

The Umm ar Rummf copper prospect, located about 30 km east of Al Qunfudhah, Kingdom of Saudi Arabia, consists of zones of malachite disseminations and fracture fillings in outcrops of north-trending impure quartzite of the Bahah group. Systematic Crone electromagnetic and self-potential surveys indicate that weakly conductive tabular bodies having a weak to moderate self-potential effect extend downdip from two discontinuously exposed, parallel ridges of mineralized quartzite. Crone electromagnetic data were quantitatively interpreted using characteristic parameter lines adapted for use at 1830 and 5010 Hz, the frequencies employed at Umm ar Rummf. Depths to the top of the conductors were computed to be from 20 to 40 m or about the thickness of the oxidized zone, which behaves as a variably conductive overburden. Both tabular conductors can also be traced geophysically to the north and south of the copper-bearing outcrops. The association of the geophysical anomalies with copper-mineralized rocks has been proved by drilling.

Reconnaissance MAXMIN electromagnetic profiles across the target using a wide coil separation show broad, low-amplitude anomalies that may indicate mineralized rocks at depth, and reconnaissance ground-magnetic profiles show strong total-field intensity anomalies associated with basaltic dikes of probable Tertiary age. In the central part of the area of investigation, these dikes produce large disturbances of the electrical fields.

INTRODUCTION

This report presents the data from and an interpretation of detailed Crone electromagnetic (CEM) and self-potential (SP) surveys of the Umm ar Rummf copper prospect, which is located near the western margin of the Arabian Shield at lat 19°09'28" N., long 41°22'36" E. (fig. 1), about 30 km east of Al Qunfudhah and 13 km west of the village of Suq al Khamis. Since 1978 the prospect has been the target of an exploratory geological, geophysical, and drilling program undertaken

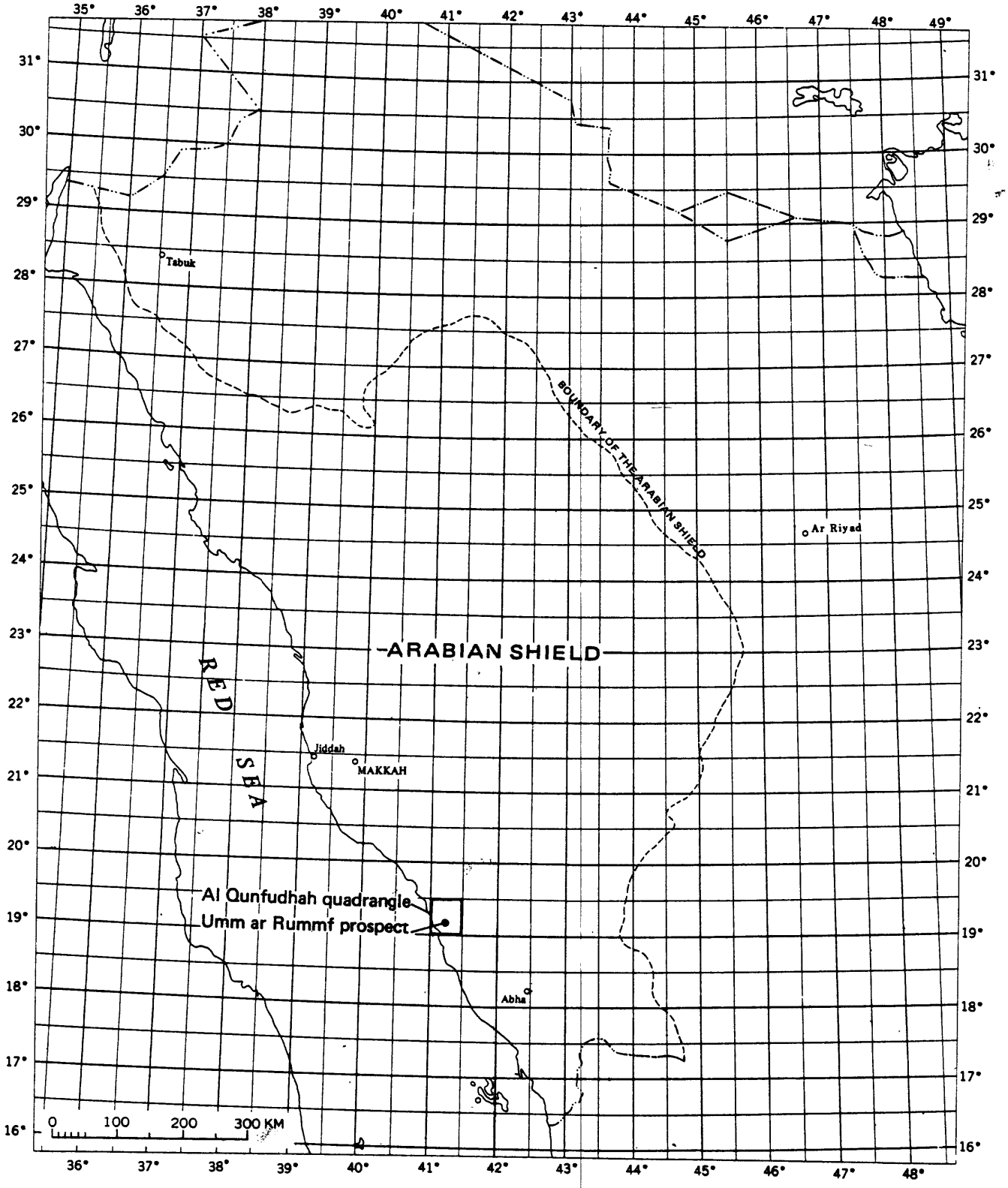

Figure 1.--Index map of western Saudi Arabia showing location of Al Qunfudhah quadrangle and Umm ar Rummf prospect.

by the U.S. Geological Survey (USGS) Saudi Arabian Mission with the aim of providing a preliminary evaluation of its copper potential, in accordance with a work agreement between the USGS and the Saudi Arabian Ministry of Petroleum and Mineral Resources. The Umm ar Rummf prospect (MODS02801) has been entered into the Mineral Occurrence Documentation System (MODS) data bank, maintained by the Saudi Arabian Deputy Ministry for Mineral Resources. Information regarding this data bank is available from the Office of the Technical Advisor, Jiddah.

Reconnaissance CEM surveys conducted over a part of the area by M. M. Mawad, C. W. Smith, and M. M. Bazzari (M. M. Mawad, unpublished data, 1978) indicate that anomalous conductivity is present, but the surveys do not provide an adequate basis for quantitative interpretation. More extensive CEM and SP surveys were later conducted, and the new results were used in conjunction with geologic and geochemical data to site three diamond drill holes, which intersected mineralized rocks below the oxidized zone (plate 1, fig. 10; also, see Mawad, unpub. data, 1982). MAXMIN electromagnetic (EM) and ground-magnetic traverses were subsequently made along three survey lines in order to help evaluate EM response patterns that might be attributed to basaltic dikes intersected in the drill holes.

The detailed CEM survey data, totaling about 7 line-km of traverse at two frequencies (1830 and 5010 Hz), are presented as profiles and contour maps having 2-degree contour intervals (plates 2-4). These data demonstrate the existence of two parallel, north-trending, weakly conductive tabular bodies, whose tops are between 20 and 40 m deep, in zones parallel to and immediately east of the exposed copper-mineralized rocks. The SP data, totaling about 10 line-km, are presented as a contour map having a 10-mV contour interval (plate 6). This map reveals that weak SP effects are associated with the conductors. Thus the conductors are interpreted to be copper sulfide disseminations localized along the dip planes of the outcropping mineralized layers. Subsurface continuations of both conductive zones are shown from the geophysical data to extend north and south from the area of mineralized outcrops. The MAXMIN and ground-magnetic data were each obtained from only 1 line-km or less of traverse and are presented as profiles (figs. 11-13).

Geology and previous work

The Umm ar Rummf prospect is in the southeastern part of the Al Qunfudhah 30-minute quadrangle (sheet 19/41 C), which was mapped by Hadley (1975). Metamorphic rocks in this region have been assigned to the Upper Proterozoic Baish and Bahah groups. The Baish group is comprised mostly of metabasalt and metamorphosed basaltic pyroclastic rocks. The

principal rocks of the overlying Bahah group are marble, slate, siliceous graywacke, argillite, chert, and conglomerate and biotite, muscovite, chlorite, siderite, and graphite schists, with subordinate metavolcanic rocks. All Precambrian strata within the area of this report are metasedimentary rocks assigned to the Bahah group; however, Umm ar Rummf itself, an area of low hills immediately east of the prospect, is composed mostly of Baish metavolcanic rocks. The contact between the Baish and Bahah groups in the Al Qunfudhah quadrangle is believed by Hadley (1975) to be conformable, although elsewhere it has been reported to be disconformable (Schmidt and others, 1973).

Near Umm ar Rummf the layered rocks trend uniformly north and dip from 60° to 65° E. However, they are situated on the eastern limb of a major regional syncline (Hadley, 1975), and the east dips must be attributed to drag folding, which according to Hadley is not uncommon in the Bahah group, or to some other tectonic process that would produce asymmetrical attitudes and westward tilting of fold-axial planes.

Mineralized rocks in the vicinity of Umm ar Rummf were first recorded by Earhart (1969?), who made an economic reconnaissance of the Suq al Khamis area. It is not certain if Earhart actually visited the site of the present investigation, because his nearest reported sample site (37165) is about 1 km east of the prospect; however, numerous mineralized zones in the eastern part of the Al Qunfudhah quadrangle and the western part of the adjacent Wadi Yiba quadrangle are indicated on his 1:64,000-scale geologic reconnaissance map of the Suq al Khamis area. These and other deposits in the area can be regarded as a southern extension of the Wadi Bidah mineral belt (Greenwood and others, 1974).

Umm ar Rummf was singled out as an exploration target by C. W. Smith and M. M. Mawad of the USGS after their discovery in 1978 of several long, narrow copper-impregnated quartzite ridges in the low-lying alluviated terrain adjacent to the Umm ar Rummf hills. No evidence was seen that would indicate that this prospect was worked in ancient times.

A geologic map of the prospect area was prepared by Mawad (unpub. data, 1982) and is reproduced here as plate 1. Mawad (unpub. data, 1982) distinguished three lithologic units within the Bahah group: monomictic metaconglomerate with quartz pebbles, fine-grained impure quartzite grading to arkose, and mineralized chloritic quartzite. These rocks have been metamorphosed mostly to quartz-sericite schist. In addition, two east-trending basaltic dikes transect the layered sequence in the middle of the map area. The similarity of their composition and habit to those of numerous mafic dikes of the Red Sea margin (Hadley, 1975; Blank, 1977) suggests that they are Tertiary in age. Much of the area mapped by Mawad (unpub. data, 1982) is overlain by

Holocene alluvium and eolian sand. Several strike-slip faults were delineated by Mawad; these trend generally easterly, transverse to metamorphic layering, and have produced small stratigraphic offsets.

Mineralization in the oxidized zone at Umm ar Rummf consists chiefly of malachite, which occurs as fracture fillings and disseminations, largely confined to the two discontinuous, nearly parallel layers of quartzite that crop out as ridges. Each mineralized quartzite layer is as wide as 5 m, and the exposed strike length of the ridge system is about 0.6 km. A geochemical survey conducted by Mawad (unpub. data, 1972), using analyses of chip and sediment samples collected at 20-m intervals along grid lines spaced 40 m apart, showed two belts of copper, lead, and zinc anomalies (pl. 1) and led to the recognition of the eastern mineralized zone. In outcrop extent this zone is much less prominent than the western zone. The geochemical traverses did not extend south of line 0 at lat 19.6° N. nor did they cover the eastern part of the map area.

No geophysical exploration was carried out at Umm ar Rummf prior to commencement of Mawad's study, although at various times both the USGS and the Riofinex Geological Mission have identified potential targets for an airborne electromagnetic (AEM) "INPUT" survey within the Al Qunfudhah quadrangle. The Umm ar Rummf area adjoins but is not included in the so-called "pyroclastic pile" block of a helicopter electromagnetic survey of the Suq al Khamis area conducted by Sander Geophysics Limited in 1968. It is about 6 km south of and nearly on strike with a strong AEM anomaly identified by that survey (Sander Geophysics Limited, unpublished data, 1968). Ground followup of this anomaly by Flanigan (1970), using a TURAM EM system, resulted in delineation of a narrow zone of anomalously high conductivity at shallow depth, but subsequent diamond drilling failed to find mineralized rocks, and it was concluded that the anomaly is associated with saline ground water localized in a shear zone.

Plan of survey

The bulk of the fieldwork for the geophysical surveys of this study was done during the period from December 25, 1979, to January 25, 1980, by Sadek with the assistance of Mohamed Nur. During this period, traverse lines were laid out and the Crone electromagnetic (CEM) and self-potential (SP) surveys were conducted. The MAXMIN EM and ground-magnetic surveys were carried out in March 1980.

The set of traverses constructed by Mawad for preliminary geologic mapping and geochemical sampling was considerably enlarged to cover the entire area with a grid suitable for

the geophysical surveys. This was done in collaboration with Mawad and included extension of his original traverses as well as the construction of 15 additional traverses, 5 to the south of the original traverses and 10 between them. All traverses of the modified set are perpendicular to Mawad's north-south base line, which lies directly west of the most prominently exposed copper-mineralized rocks. The grid net has the following specifications:

1. Traverse direction: east-west
2. Average length of traverse: 340 m
3. Traverse spacing: 20 m (line 0 to 200 N) and 40 m (elsewhere)
4. Station spacing along each traverse: 20 m

The entire set of lines, including the base line, was laid out by simple chain and compass. However, it was necessary to resurvey the three lines later selected for MAXMIN work by the method of secant chaining.

GEOPHYSICAL EQUIPMENT AND SURVEY TECHNIQUES

Crone electromagnetic survey

Standard electromagnetic exploration methods, including Crone electromagnetic surveying (CEM) are based on the fact that when an electrical conductor is subjected to a primary alternating field, a secondary current is induced in the conductor; the current develops a secondary alternating field, which together with the primary field produce a resultant field of different amplitude and phase from the applied primary field. These differences are measured by the CEM unit as dip angle (tilt) and phase lag or lead, which can be interpreted to yield the probable location and strength of subsurface conductors. The equipment employed in the Umm ar Rummf survey was manufactured by Crone Geophysical Company, Limited, of Canada and consists of two identical transceiver coils tuned to frequencies of 390, 1830, and 5010 Hz. Each coil is used first in either a transmitter or receiver mode while the other coil is used in the complementary mode; hence the system is referred to as a "shootback" system. By interchanging the roles of the coils during each set of measurements and averaging the results, the effects of elevation difference between the transmitter and receiver are eliminated; thus the CEM system, which requires no hardwire connection between the two coils, is ideally designed for rapid reconnaissance. The actual field measurements are carried out by fixing the orientation of the transmitter and then

rotating the receiver until a null is observed on a field-strength meter. An audio null is also found using crystal headphones.

The CEM survey is carried out along traverses perpendicular to the strike of the target conductors, by using one or more coil spacings and frequencies. The system can be used in four modes: 1) horizontal shootback (plane of transmitter coils horizontal, plane of receiver coils vertical and perpendicular to line of traverse); 2) coaxial or "JEM" shootback (transmitter coils vertical and coaxial with receiver coils, along line of traverse; this method reduces coupling to the surface); 3) vertical loop (coils vertical and coplanar); and 4) horizontal loop (coils horizontal and coplanar). Details of the CEM method are given in Telford and others (1976).

Determination of survey parameters

A test survey was conducted first along line 120 N (see plate 2 for location), using all three frequencies, several coil separations, and both shootback modes, in order to choose the optimum values to be used during the survey. Traverse line 120 N was chosen because on the earlier reconnaissance survey by Mawad the maximum registered dip angle was recorded over station 40 E of this traverse. The results of this test survey at a 40-m coil spacing and 390 Hz frequency, using two coil configurations (horizontal and coaxial shootback), are given in table 1. Only a weak response was obtained for either configuration, especially the coaxial mode, which showed considerable noise. A second test survey was conducted along the same traverse line using the horizontal-shootback mode at an 80-m coil spacing and frequencies of 1830 and 5010 Hz. The results of this test survey are given in table 2. These data show better delineated anomalies, having dip angles of as much as -20° over station 60 E at 5010 Hz and -12° at 1830 Hz. All dip-angle values were negative, which is attributable to the effect of a relatively thick conductive overburden (weathered zone), as will be described later.

Finally, a third test survey was carried out using horizontal shootback at coil spacings of 40, 60, 80, and 100 m and frequencies of 390, 1830, and 5010 Hz over stations 40, 60, and 80 E, that is, across the region of maximum response for 80-m coil spacing. The results of this survey are given in table 3. These data show that an 80-m coil spacing and frequencies of 1830 and 5010 Hz provide the optimum response. Accordingly, the horizontal-shootback mode and the above parameters were selected for the survey.

Table 1.--Crone electromagnetic (CEM) tilt and out-of-phase measurements along line 120 N, using 40-m coil spacing and horizontal- and coaxial-shootback modes

[Leader indicates no data available]

Station[1]	Shootback mode			
	Horizontal			Coaxial
	1830 Hz		390 Hz	1830Hz
	Out-of phase[2]	Tilt[3]	Tilt[3]	Tilt[3]
100 W	5	-	-	-
80 W	6	+2	+2	+1
60 W	6	+3	+3	-1
40 W	8	+4	+3	-2
20 W	6	0	0	0
0	6	-4	-2	+1
20 E	6	+3	+1	+1
40 E	4	+2	+2	-2
60 E	3	-4	-2	-1
80 E	7	-1	+1	+1
100 E	6	-3	+3	0
140 E	5	-1	-2	-1
160 E	7	+3	-3	-2
180 E	6	+4	+4	+2
200 E	-	+2	+3	+1

1/ Station location is midpoint of coil pair for tilt measurements and location of receiver station for out-of-phase measurements (out-of-phase read only once for each pair of tilt readings).

2/ Out-of-phase measurement (in percent) is the ratio of strength of quadrature component to strength of normal (undisturbed) field.

3/ Tilt angle (in degrees) represents the algebraic sum of the two tilt angles: the tilt angle of the coil is measured below the horizontal when the coil is in the receiver mode, then the two tilt angles are summed.

Table 2.--Crone electromagnetic (CEM) horizontal-shootback tilt measurements along line 120 N, using 80-m coil spacing and frequencies of 1830 and 5010 Hz

[Tilt is in degrees; station location is midpoint of coil pair]

	1830 Hz	5010 Hz
Station	Tilt	Tilt
60 W	- 8	-17
40 W	- 3	- 9
20 W	- 9	-16
0	- 4	-10
20 E	- 2	- 6
40 E	- 5	-10
60 E	-12	-20
80 E	-18	-16
100 E	- 2	- 6
120 E	0	- 4
140 E	- 8	-14
160 E	- 3	-13
180 E	- 8	-12
200 E	- 7	-11

Table 3.--Crone electromagnetic (CEM) horizontal-shootback tilt measurements along line 120 N for three stations directly east of exposed copper-mineralized rocks, showing effect of coil spacing

[Frequency in Hz; tilt in degrees. Station location is midpoint of coil pair]

Coil spacing	40 m			60 m			80 m			100 m		
	Tilt			Tilt			Tilt			Tilt		
Frequency / Station	390	1830	5010	390	1830	5010	390	1830	5010	390	1830	5010
40 E	+2	+1	+2	+3	-1	-3	-1	- 4	-10	- 3	- 5	-14
60 E	+3	+2	+4	-3	0	-5	+2	-11	-20	- 5	- 8	-26
80 E	0	-1	+3	+3	-3	-5	-8	- 8	-16	- 3	-10	-17

Self-potential survey

The self-potential (SP) method is well known, and the technique is explained in most geophysical textbooks. SP surveying provides a fast and efficient exploration tool for massive and disseminated sulfide bodies, although it may have less resolving power than CEM surveying and commonly is more difficult to interpret quantitatively. In the present survey an electronic millivoltmeter (model PS-4) obtained from the Bureau de Recherches Geologiques et Minieres of France was coupled to two porous-pot electrodes filled with a uniform batch of saturated copper sulfate solution. The survey was conducted using the fixed-electrode method; station 20 N, 140 W was chosen as the fixed point and reference base. This station is located on a small hill formed by outcrops of quartz-vein material and has a positive SP value relative to most other grid stations.

MAXMIN electromagnetic and ground-magnetic surveys

MAXMIN surveying is a "slingram" or horizontal-loop EM system manufactured by APEX-Parametrics Limited of Canada. It employs coplanar transmitter and receiver coils separated by a fixed distance and connected by cable. In-phase and out-of-phase (quadrature) field strength are measured with respect to the transmitted signal. Both coils must be carefully oriented before each reading. MAXMIN surveying has a higher power output and can be used for greater depths of exploration than CEM surveying but is slower and more costly to operate, especially in areas of rough topography where it is generally necessary to employ a method such as secant chaining to establish the proper orientation.

Of the five frequencies (111, 222, 444, 888, and 1777 Hz) available with the instrument used (MAXMIN model III) only the highest two proved effective. The survey used a coil separation of 150 m and station intervals of 20 m along the profiles.

A Geometrics model G-816 total-field proton magnetometer was used for the ground-magnetometer traverses, which were conducted along the three lines selected for the MAXMIN survey. Readings were taken at 20-m intervals along the lines. All station readings were corrected for diurnal drift and reduced relative to an average value assumed for the base station (39,168 nT at station 220 W, line 120 N).

CRONE ELECTROMAGNETIC SURVEY RESULTS

Qualitative interpretation

An examination of the CEM profiles (plate 2) and contour maps (plates 3 and 4) leads to the following observations:

1. Two major anomalous zones, labeled A and B on the maps, can be easily identified. These zones trend approximately north and are separated by a distance of approximately 100 m. The relatively smooth anomaly trends within the zones are interrupted in the vicinity of the transverse basaltic dikes mapped by Mawad (unpub. data, 1982).

2. Zone A consists of anomalous values between stations 100.E and 140 E on the traverses and seems to be continuous except on lines 80 N and 60 N (plates 3 and 4), where the anomaly trends intersect the east-trending dike. After the southern part of this zone (south of line 60 N) was delineated, geological mapping was extended and a thin stratum of mineralized quartzite trending parallel to the axis of the anomaly was discovered between 10 and 20 m west of the anomaly peak. Although no copper-mineralized rocks have been found in association with anomalous zone A north of line 60 N, it seems reasonable to interpret the entire zone as the expression of a buried weak conductor produced by mineralized rocks along the strike- and dip-extension of the exposed copper-bearing quartzite bed.

Zone B, on the other hand, consists of anomalous readings obtained between stations 20 W and 20 E on the traverses. It is apparently offset by several small strike-slip faults. It also has a discontinuity on lines 100 N, 80 N, and 60 N in the vicinity of the east-trending basalt dikes. South of line 0 this anomaly resumes a more regular character but is nevertheless weak and diffuse and is not associated with mineralized rocks. The northern, well-delineated part of zone B is clearly associated with mineralized quartzite outcrops located from 20 to 40 m west of the anomaly crest. However, a few meters east of the base line between lines 40 N to 120 N, in an area where the mineralized bed is thickest and forms a prominent ridge, zone B is discontinuous and complex. The complexity of the anomaly pattern at this location may result partly from conductive wadi sediments, but the principal reason for disruption of the pattern is most likely the existence of the east-trending basaltic dike system and its effect on the distribution of saline ground water.

Both zones appear on the map at each frequency (plates 3 and 4), although in the central part of the 1830-Hz map, zone B is predominant.

3. The dip-angle anomalies (plate 2) have a relatively weak central high flanked by lows of comparable amplitude. Their shapes and relative amplitudes are similar to those of model curves given by Crone (unpublished data, 1972) for thin tabular conductors (fig. 2). Because the mineralized zone is no wider than 5 m at the outcrop, a thin-sheet model seems appropriate. Thus, by comparison with the Crone curves (fig. 2), the probable depth to the top of the conductors at Umm ar Rummf is between 0.25a and 0.5a. The factor "a" is the coil spacing, which in this case is 80 m, and thus the depth of the top of the conductor is between 20 and 40 m.

4. The datum for the anomalies is clearly negative (plate 2), neither shoulder of any anomaly reaching zero. This is attributable to conductive overburden and interference with other anomalies. The effect of overburden was described by Crone (unpublished data, 1972) and is illustrated in figure 3. Uniformly conductive overburden simply lowers the datum, the amplitude of the effect varying in response to changes in thickness. This effect occurs with either the horizontal-shootback or coaxial-shootback ("JEM") mode.

5. If the negative datum of the Umm ar Rummf anomalies is taken into consideration, a standard thin-sheet model no longer suffices and it is evident that the anomalies more nearly match those produced by dipping dikes beneath conductive overburden, an example of which is given in figure 4. This anomaly was recorded over a thin conductor dipping 55° and buried beneath approximately 15 m of conductive clay. The depth of burial for conductors at Umm ar Rummf implied by comparison with the example of figure 4 agrees with the depth deduced from consideration of only the shape and amplitude of the field curves, ignoring the datum shift.

Quantitative interpretation

Quantitative interpretation of Crone electromagnetic and other electromagnetic data is complex because many factors affect the shape and amplitude of a recorded anomaly. These factors include the depth to the top of the conducting body, the conductivity-thickness product (conductance) and geometrical configuration of the body, the conductivity of the overburden and host rocks, and the frequency, geometry, and scale of the probing array. Moreover, the detected anomalies are commonly the combined response of more than one conductor. Although standard curves for interpretation of sheetlike-conductor anomalies detected by the vertical- and horizontal-loop methods have been available for many years, the Crone electromagnetic-shootback method is a relatively new development and few procedural guides for the quantitative treatment of CEM data have been assembled. The most important study in addition to those by the developer (Crone, 1966 and unpublished data, 1968, 1972) is by Lin (1969).

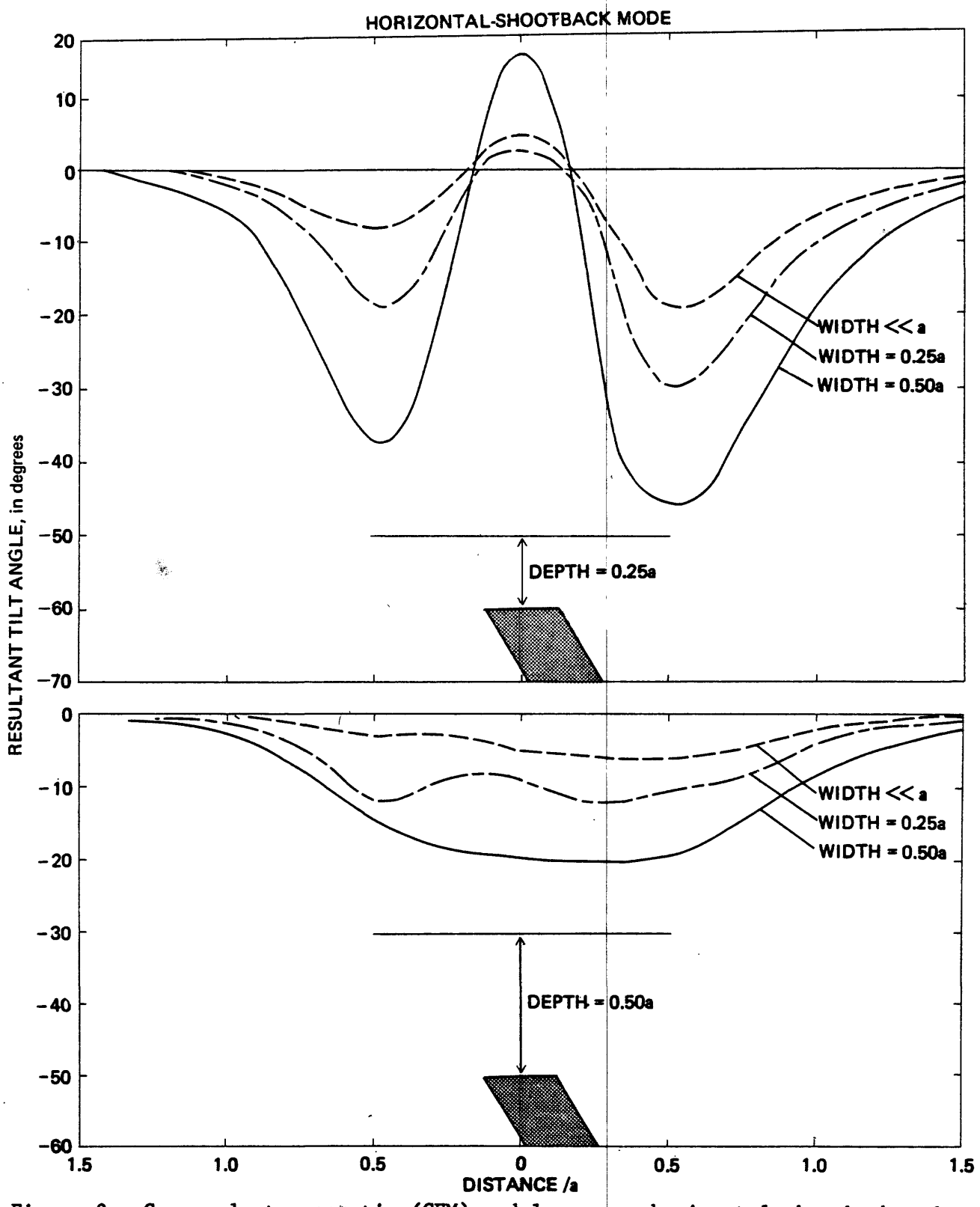

Figure 2.--Crone electromagnetic (CEM) model curves, horizontal-shootback mode, showing response of tabular conductor dipping 60°, for various widths and two depths of burial (after Crone, unpublished data, 1972). a = coil spacing; reading at midpoint between coils; infinite conductivity.

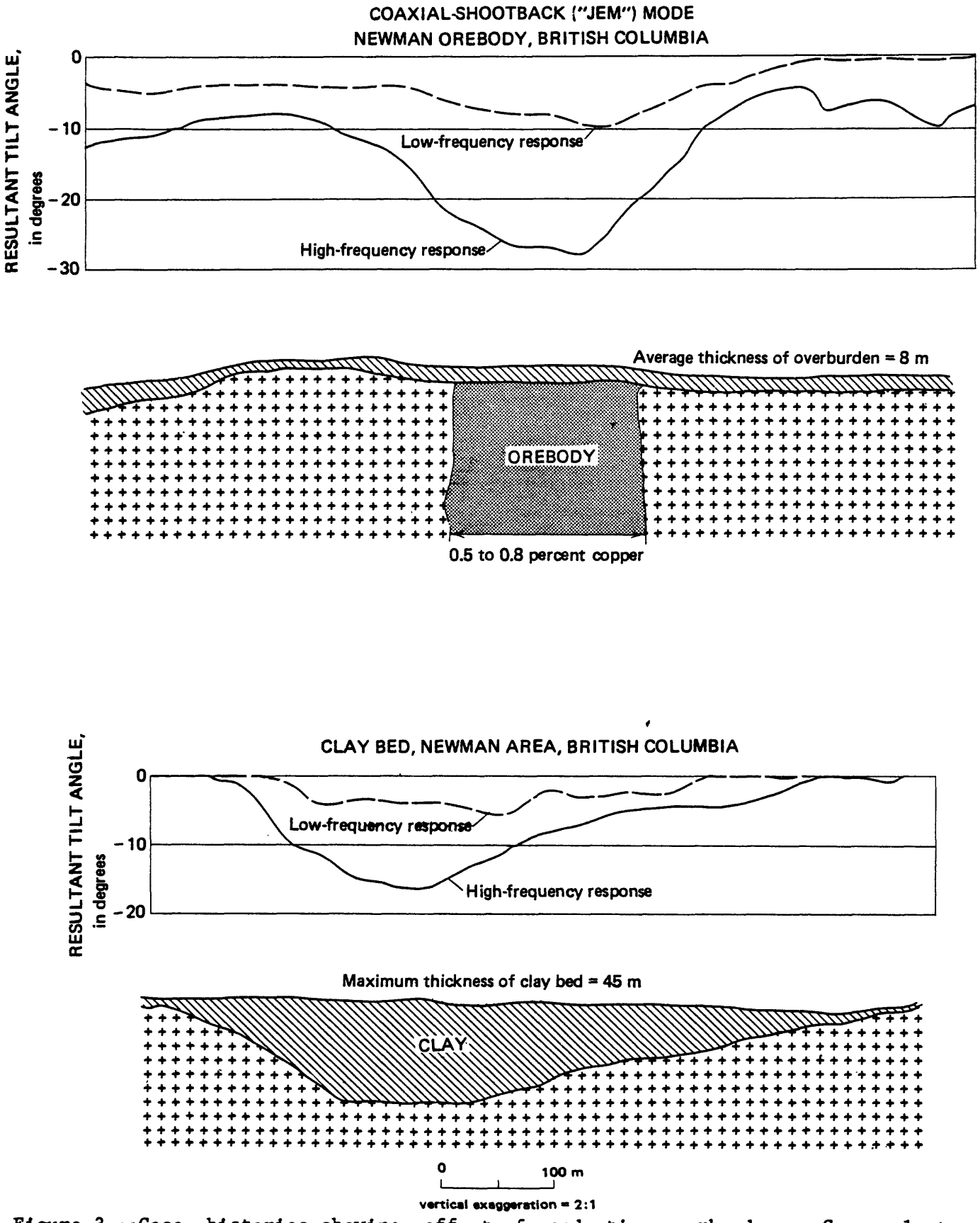

Figure 3.--Case histories showing effect of conductive overburden on Crone electromagnetic (CEM) response, coaxial-shootback mode, Newman area, British Columbia (after Crone, unpublished data, 1972). Dashed line = low-frequency response; solid line = high-frequency response.

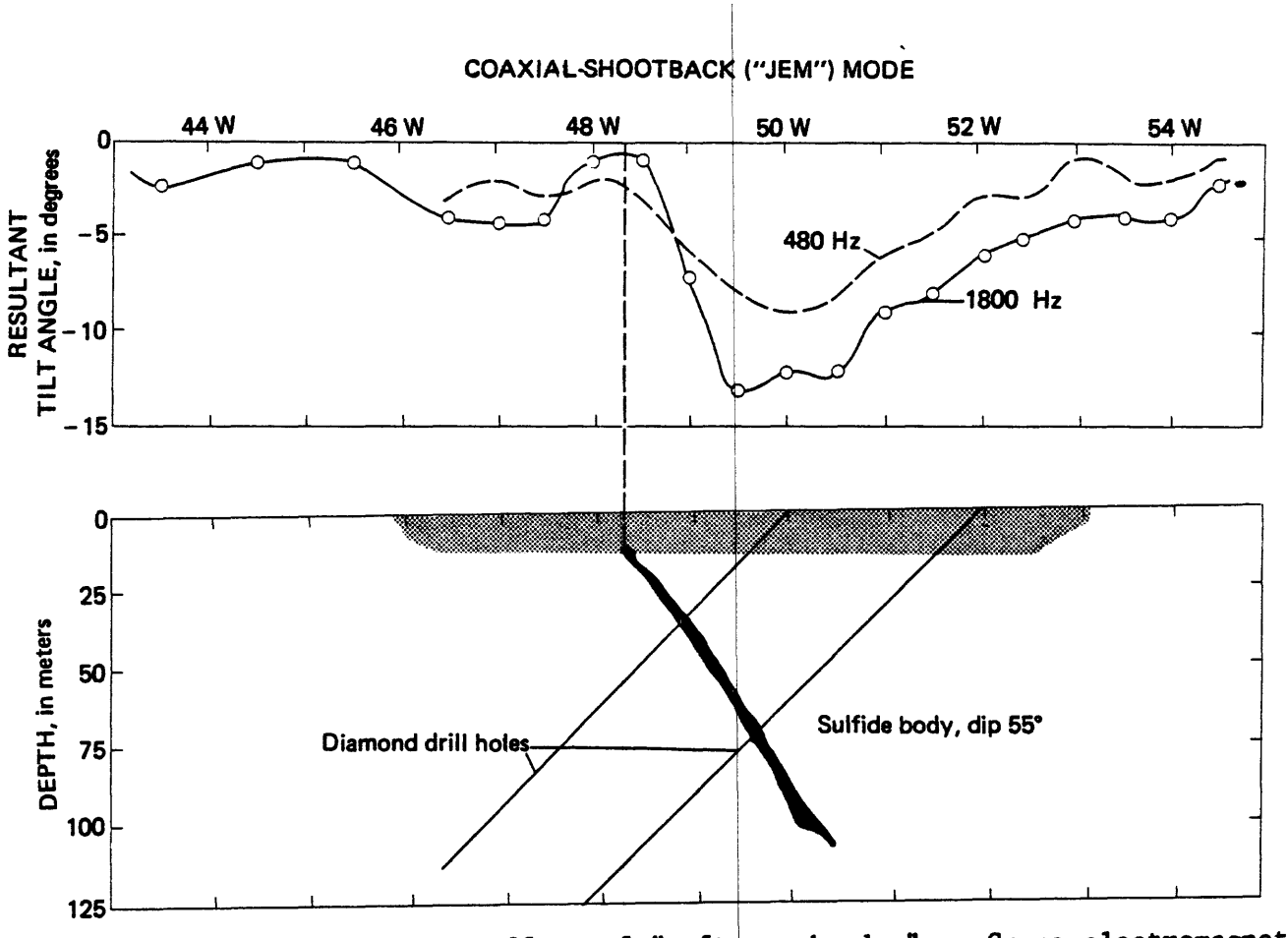

Figure 4.--Case history showing effect of "soft overburden" on Crone electromagnetic (CEM) response, coaxial-shootback mode, for a dipping sulfide body, Timmins area, Ontario (after Lin, 1969).

Lin (1969) carried out a series of model experiments for dipping sheetlike conductors embedded in a homogeneous half-space and studied the effect of systematic variations in target characteristics on parameters that can be measured directly from the resulting anomalies. The typical anomaly of a dipping dike has two troughs flanking a central crest, which is located over the apex of the body. Lin empirically determined the relationship between the relative amplitudes of the two anomaly troughs and the dip of the target. He then showed how measurement of anomaly parameters at two different frequencies f_1 and f_2 can be used to determine conductance and depth of burial for dikes of a given attitude.

In order to use Lin's (1969) method of interpretation in our study, his plots were converted to the corresponding plots for frequencies available with our particular CEM system. This operation was carried out by Sadek and resulted in the interpretation plots of figures 5 through 8.

The parameters used in quantitative interpretation of the field-anomaly curves by Lin's (1969) method are as follows (see figure 9).

a = coil spacing

H = horizontal distance between negative peaks

α_{max} = amplitude of larger trough

α_{min} = amplitude of smaller trough at the same frequency

$\Delta\alpha = \alpha_{max} - \alpha_{min}$

$\alpha_1 = \alpha_{max}$ at frequency f_1

$\alpha_2 = \alpha_{max}$ at frequency f_2 ($f_2 > f_1$)

Using this notation, the step-by-step procedure for quantitative interpretation of the anomalies is as follows:

1. Identify all discrete anomalies of both zones A and B and number them serially (plate 2).

2. Measure H, α_{max}, and α_{min} at f_1 (1830 Hz).

3. Measure H, α_{max}, and α_{min} at f_2 (5010 Hz).

4. Calculate the quantity $\Delta\alpha/\frac{H}{a}$ at 5010 Hz (the higher frequency yields higher anomaly amplitudes).

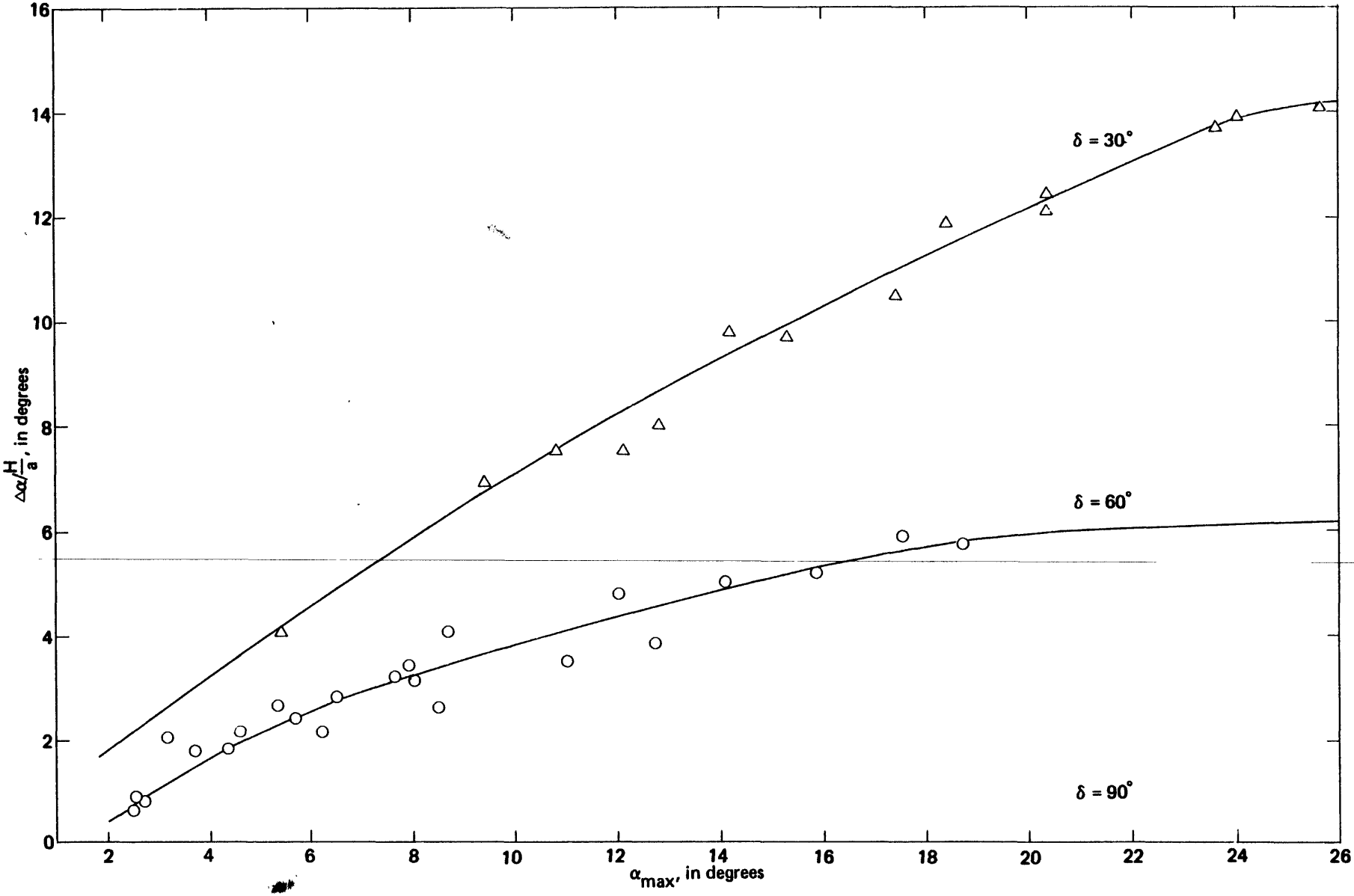

Figure 5.--Plot of $\Delta\alpha/\frac{H}{a}$ versus α_{max} used for determining dip of conductor (after Lin, 1969). H = horizontal distance between anomaly troughs (minima); a = coil spacing; $\Delta\alpha$ = difference in amplitudes of the two minima; α_{max} = amplitude of larger trough (minimum)(in degrees); δ = dip of thin tabular conductor (in degrees).

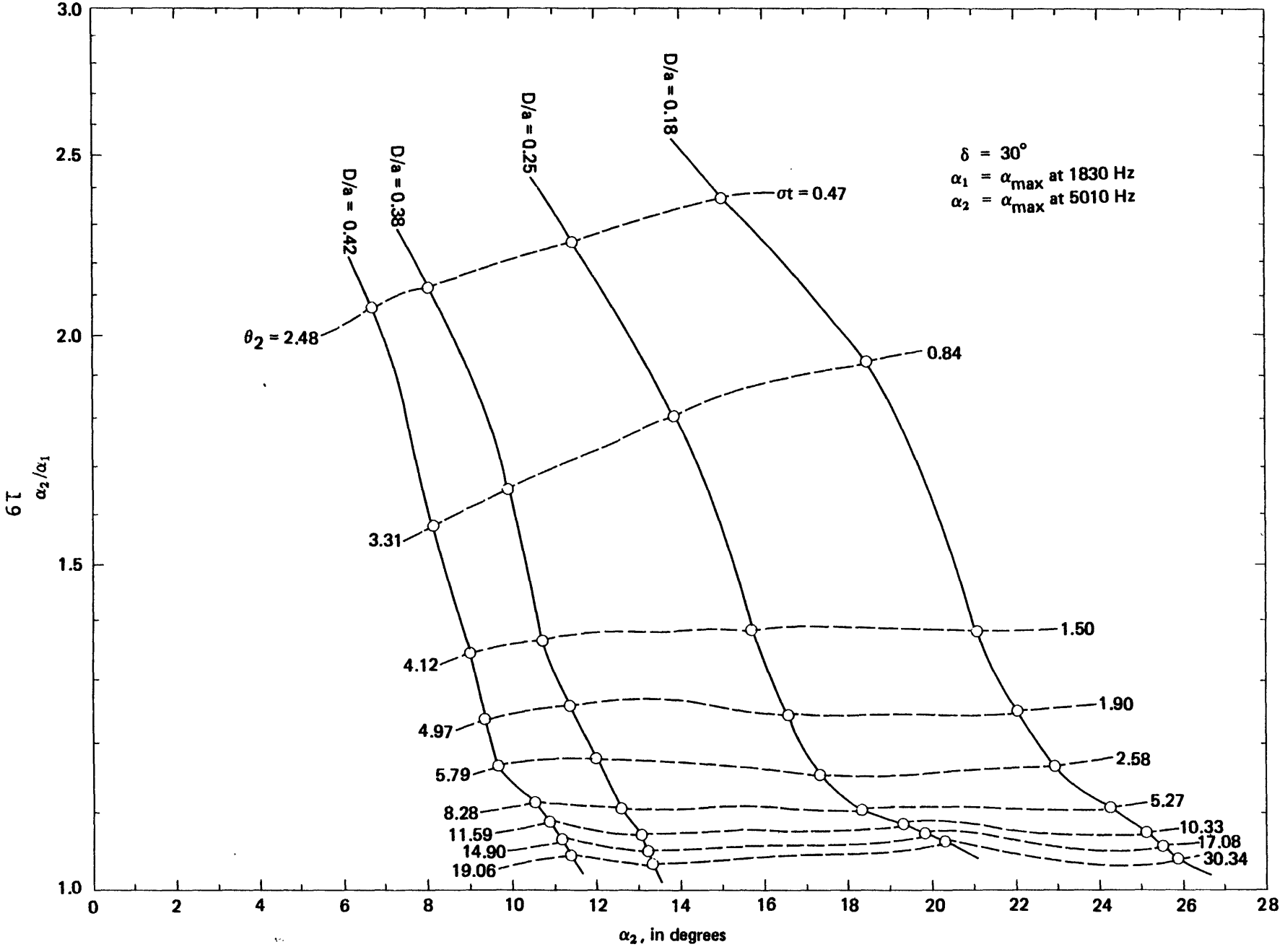

Figure 6.--Characteristic curves for determining the depth and conductance of a thin tabular conductor, which has a dip of 30°, at frequencies of 1830 and 5010 Hz (calculated from data of Lin, 1969). α_{max} = amplitude of larger trough (minimum)(in degrees); D = depth of burial; a = coil spacing; σ = conductivity (in mho-meters); t = thickness of conductor; σt = conductance (mho); θ_2 = induction number.

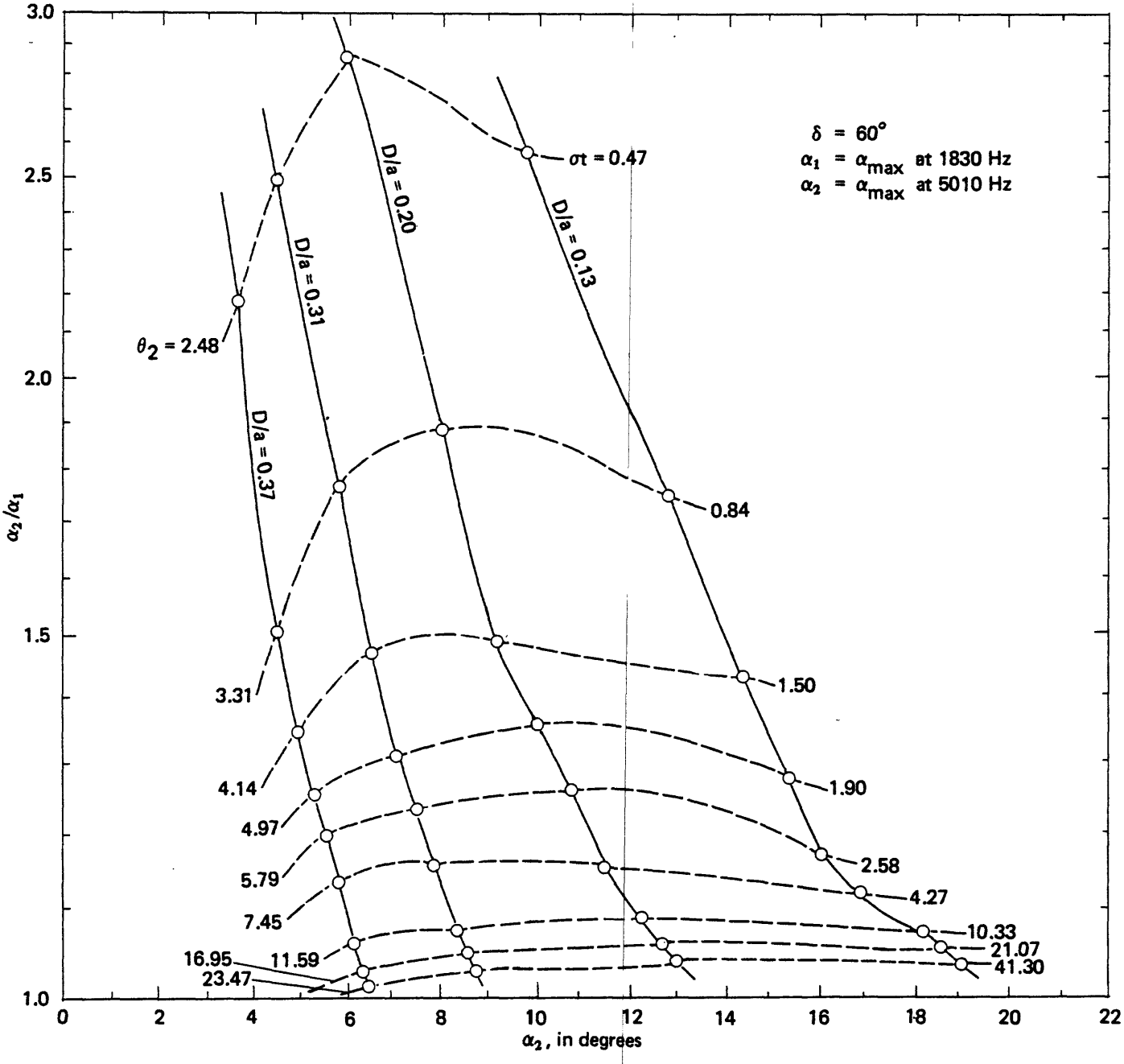

Figure 7.—Characteristic curves for determining the depth and conductance of a thin tabular conductor, which has a dip of 60°, at frequencies of 1830 and 5010 Hz (calculated from data of Lin, 1969). α max = amplitude of larger trough (minimum)(in degrees); D = depth of burial; a = coil spacing; σ = conductivity (in mho-meters); t = thickness of conductor; σt = conductance (in mho); θ_2 = induction number.

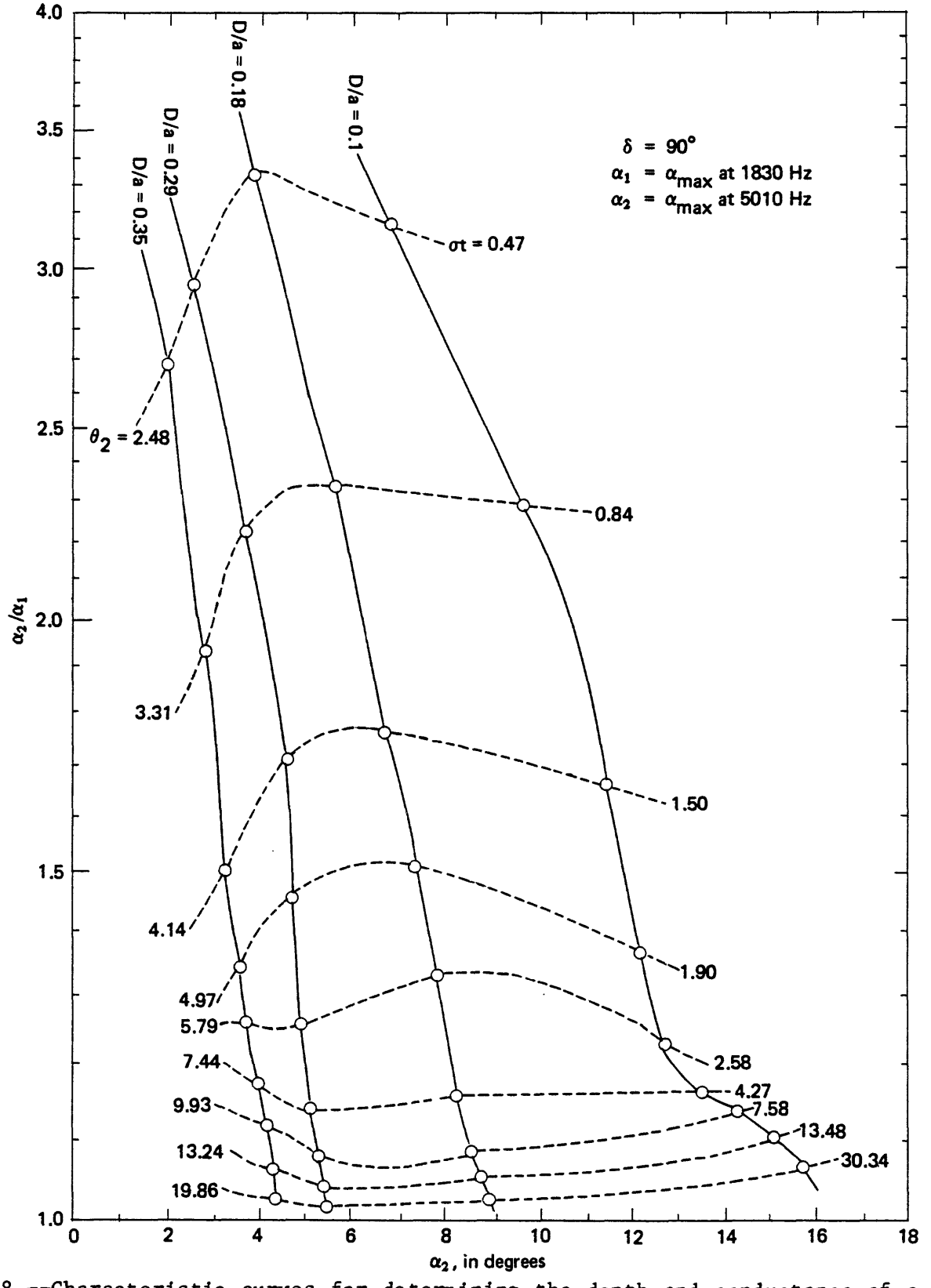

Figure 8.--Characteristic curves for determining the depth and conductance of a thin tabular conductor, which has a vertical dip, for frequencies of 1830 and 5010 Hz (calculated from data of Lin, 1969). α_{max} = amplitude of larger trough (minimum)(in degrees); D = depth of burial; a = coil spacing; σ = conductivity (in mho-meters); t = thickness of conductor; σt = conductance (in mho); θ_2 = induction number.

5. Use the plot of $\Delta\alpha/\frac{H}{a} : \alpha_{max}$ (in this case α_2; see fig. 8) to determine the dip of the tabular conductor.

6. Calculate the quantity α_2/α_1.

7. Use the plot of $\alpha_2/\alpha_1 : \alpha_2$ corresponding to the determined dip to determine the quantities D/a and σt, the depth/coil spacing ratio and conductivity-thickness product, respectively.

8. Use the coil spacing of 80 m and an assumed thickness of 5 m to obtain the depth of burial and conductivity, respectively.

The results of these operations are given in table 4. It was not feasible to analyze all the anomalies listed because in some cases the anomaly resolution (separation of adjacent anomalies) was inadequate.

The interpreted conductor dips are mostly from 60 to 70° E., in agreement with the dips determined from the mineralized quartzite outcrops. This agreement confirms the hypothesis that the mineralized zones are essentially conformable with the enclosing strata.

The calculated depth D to the top of the conductor ranges from 10 to 20 m. This depth is probably less than the true depth because the datum shift produced by the overburden increases both α_1 and α_2 equally and therefore decreases the ratio α_2/α_1. It is clear that increasing α_2 decreases the calculated depth, whereas decreasing the ratio α_2/α_1 increases the calculated conductivity-thickness product (figs. 9-11). Accordingly, the conductivity values are probably also in error and too large. Estimates of conductor depth and conductivity can clearly be improved by removal of the effect of overburden from the field curves, but this is difficult to do without better knowledge of overburden conductivity and thickness. Under the circumstances we have been content to make crude corrections to the calculated depths and to leave the calculated conductivities unchanged. Adjustment to the depth estimates are based on a qualitative evaluation of the datum shift as seen on each field curve, followed by recalculation of the crucial parameters α_1 and α_2. This procedure results in the second set of calculated depths (D') shown on table 4. The new values are from 10 to 120 percent greater than the uncorrected ones and, although admittedly very rough, are undoubtedly more realistic than those calculated directly from the observed field data. In general they agree with the thickness of the zone of oxidation as determined from drill cores.

Table 4.--Results of quantitative Crone electromagnetic (CEM) interpretations

[--, anomaly not analyzed, in most cases because of inadequate anomaly resolution. Calc dip, calculated dip. All values in degrees unless specified, except for H/a, and α_2/α_1, which are unitless]

			5010 Hz				1830 Hz												
Anomaly	Traverse	Peak location	$\Delta\alpha$	$\frac{H}{a}$	$\frac{\Delta\alpha}{H/a}$	Calc dip δ_2	$\Delta\alpha$	$\frac{H}{a}$	$\frac{\Delta\alpha}{H/a}$	Calc dip δ_1	Average dip δ	α_2	α_1	α_2/α_1	Calculated depth D (meters)	Adjuated depth D' (meters)	Calculated conductance σt (mho)	Calculated conductivity σ @ t = 5 m (mho-meters)	Remarks
1	160 S	140 E	13	2.25	5.78	62	4	2.25	1.78	70	66	-24	- 9	2.67	<10	17	<0.47	<0.09	
2	120 S	140 E	7	1.50	4.67	65	1	0.67	1.49	73	69	-22	- 9	2.44	<10	20	<.47	<.09	
3	80 S	120 E	--	--	--	--	--	--	--	--	--	-20	- 9.5	2.11	<10	18	<.47	<.09	Incomplete anomaly
4	40 S	140 E	13	1.50	8.66	47	8	1.50	5.88	40	44	-19	- 9	2.11	<15	22	.50	.10	
5	0	120 E	--	--	--	--	2	1.50	1.33	80	80	-10	- 8	1.25	16	19	2.58	.52	Incomplete anomaly
6	20 N	130 E	--	--	--	--	--	--	--	--	--	-12	- 5	2.40	<10	15	.50	.10	Incomplete anomaly
7	20 N	0	--	--	--	--	--	--	--	--	--	-15	- 9	1.67	<10	18	.80	.16	Incomplete anomaly
8	40 N	120 E	8	1.75	4.57	67	4	1.75	2.29	73	70	-20	-12	2.0	11	17	.65	.13	Incomplete anomaly
9	80 N	20 E	1	1.0	1.0	63	--	--	--	--	63	-12	- 6	2.0	11	20	.65	.13	Incomplete anomaly
10	120 N	120 E	--	--	--	--	--	--	--	--	--	-13	- 9	1.44	13	19	1.30	.26	Incomplete anomaly
11	120 N	20 E	4	1.0	4	70	3	1.0	3.0	68	69	-20	-12	1.67	10	20	.65	.13	
12	140 N	100 E	9	1.0	9	50	4	1.25	3.20	63	57	-18	-10	1.8	<10	16	.60	.12	
13	140 N	20 E	1.0	1.0	1.0	75	5	1.0	5.0	40	57	- 9	- 7	1.29	20	22	2.1	.42	
14	160 N	100 E	--	--	--	--	2	1.25	1.60	75	75	-13	- 8	1.63	10	17	.80	.16	Incomplete anomaly
15	180 N	100 E	5	2.0	2.5	80	--	--	--	--	80	-17	- 7	2.43	10	15	<.47	<.09	Incomplete anomaly
16	200 N	100 E	5	1.5	3.33	70	1	1.5	0.67	83	76	-20	- 9	2.22	10	17	<.47	<.09	
17	200 N	20 E	--	--	--	--	--	--	--	--	--	-15	- 8	1.88	10	20	.70	.14	Incomplete anomaly
18	240 N	100 E	2	1.75	1.14	80	2	1.75	1.14	75	77	-16	- 8	2.0	10	18	1.47	.09	
19	240 N	0	3.0	1.0	3.0	70	1.0	1.0	1.0	75	73	-12	- 6	2.0	10	19	.65	.13	
20	280 N	120 E	7	1.75	4.0	67	2.0	1.75	1.14	75	71	-16	- 7	2.29	10	20	.50	.10	
21	280 N	20 E	--	--	--	--	2.0	1.0	2.0	60	60	- 9	- 5	1.80	15	20	.80	.16	Incomplete anomaly
22	320 N	110 E	2.0	1.25	1.60	75	1.0	1.25	0.80	75	75	-12	- 6	2.0	10	21	.70	.14	
23	320 N	20 E	--		--	--	--	--	--	--	--	-11	- 5	2.2	11	18	.60	.12	Undefined anomaly
24	360 N	100 E	3.0	1.0	3.0	73	1.0	3.0	0.33	80	76	-16	- 6	2.67	<10	19	<.47	<.09	
25	360 N	20 E	--	--	--	--	--	--	--	--	--	-12	- 6	2.0	10	20	.65	.13	Undefined anomaly
26	400 N	90 E	6.0	1.25	4.8	60	2.0	1.25	1.6	68	65	-14	- 6	1.75	<10	22	.75	.15	
27	400 N	20 E	--	--	--	--	--	--	--	--	--	- 8	- 4	2.0	15	24	.75	.15	Undefined anomaly
28	440 N	100 E	--	--	--	--	--	--	--	--	--	-14	- 6	1.75	<10	18	.75	.15	Undefined anomaly

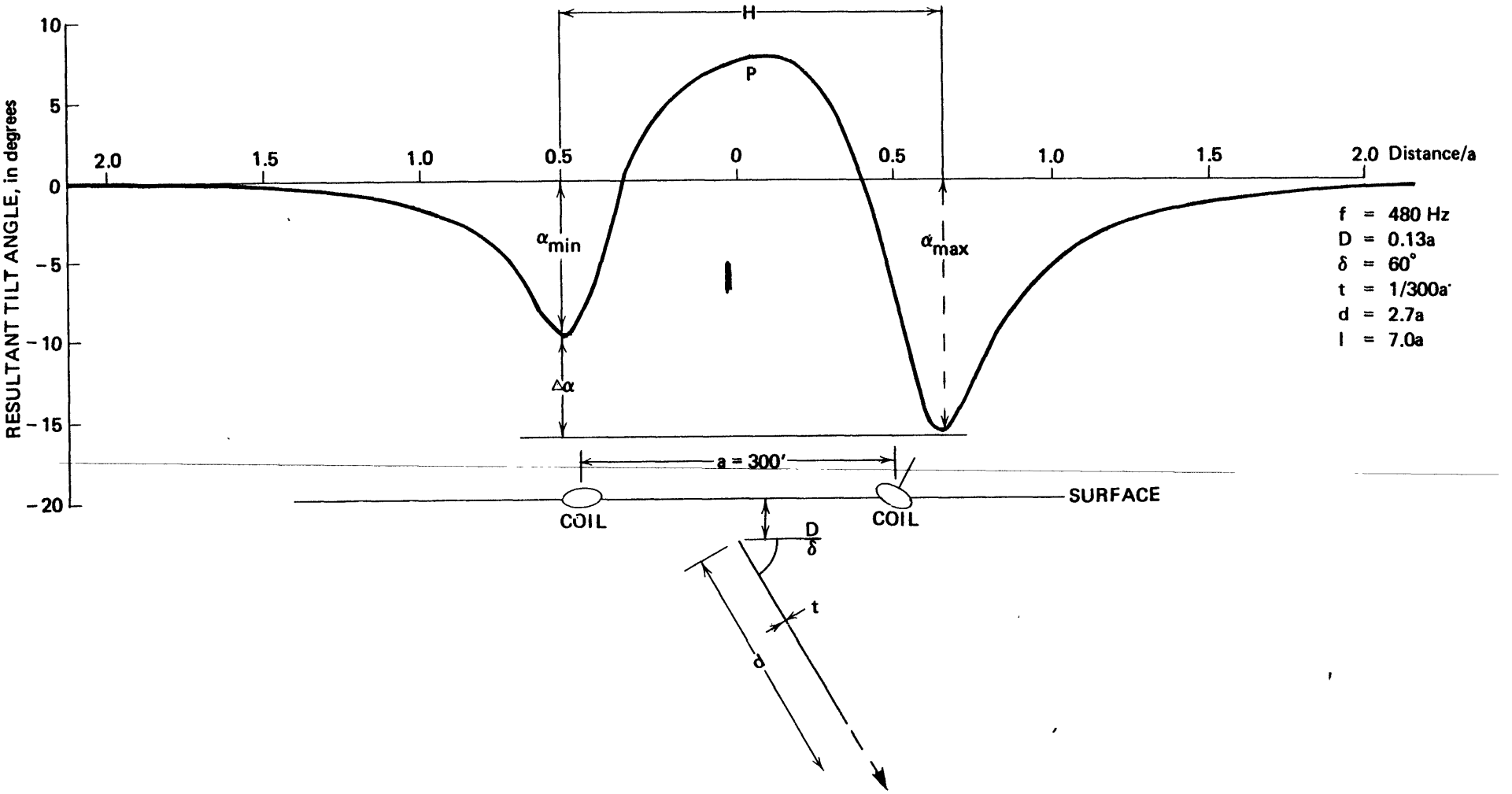

Figure 9.--Graph showing ideal Crone electromagnetic (CEM) anomaly over a dipping sheet conductor, illustrating the parameters measured in quantitative interpretation (after Lin, 1969). See text for discussion of parameters.

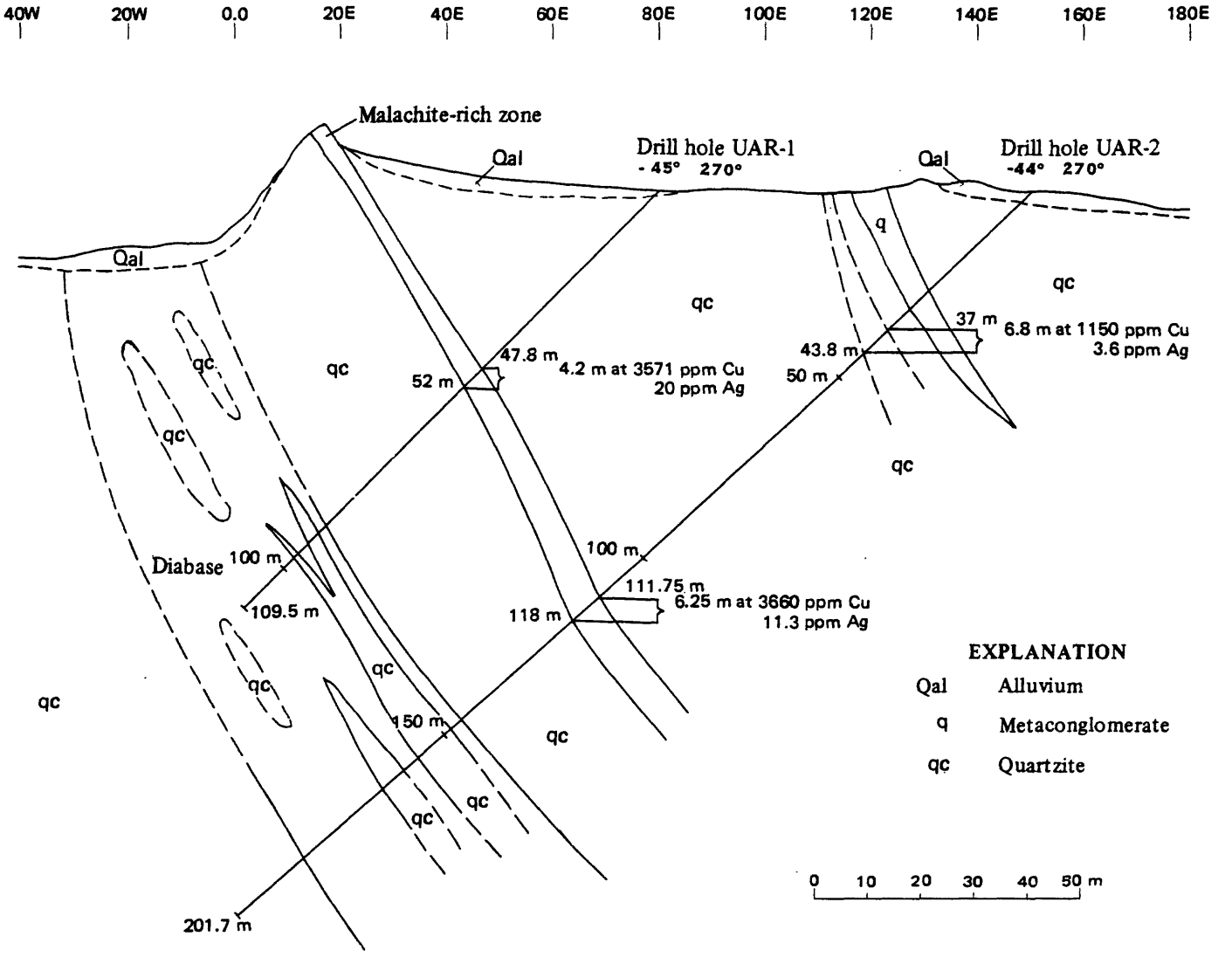

Figure 10.--Cross section of drill holes UAR-1 and UAR-2 at the Umm ar Rummf prospect (from Mawad, 1982).

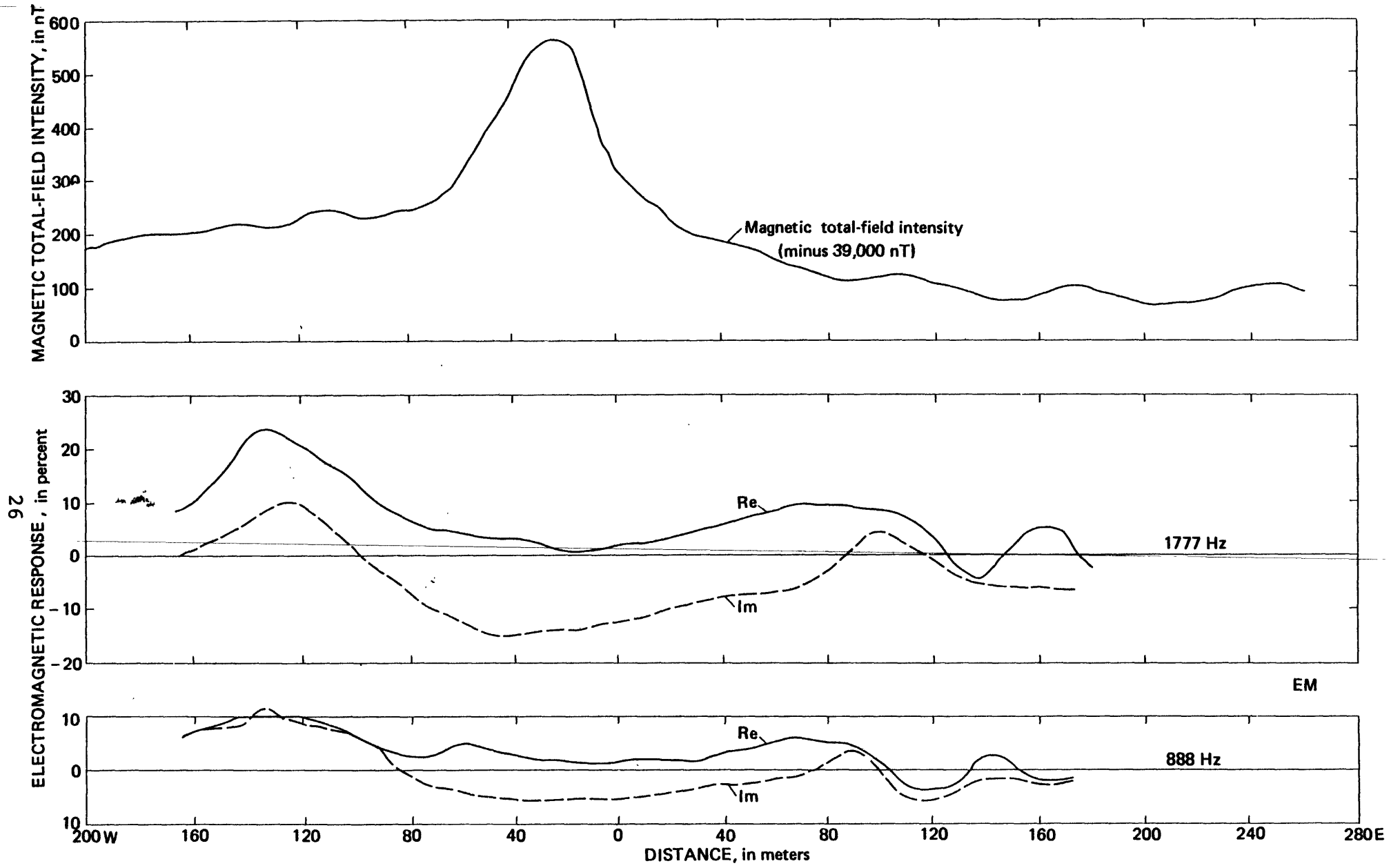

Figure 11.--Profiles showing MAXMIN electromagnetic and ground-magnetic data along line 120 N, Umm ar Rummf prospect. Re = real component; Im = imaginary (quadrature) component of anomalous (secondary) field; Re and Im given in percent of primary field at receiver. Electromagnetic coil spacing is 150 m; data point at center of spread.

The calculated conductivity ranges from 0.1 to 0.4 mho, values which indicate the target is a rather poor conductor. This is true despite the fact that the effect of overburden has been ignored in the calculations.

A map of the quantitative CEM results is given on plate 5, which depicts the location of the top of conductive zones together with interpreted depth and conductivity data. Note that the depths to top of conductor shown on this map are the adjusted values D' calculated by taking into consideration the effect of overburden.

OTHER SURVEY RESULTS

Self-potential survey

Examination of the self-potential (SP) map (plate 6) shows that the SP relief in the area of interest is relatively low. Anomalies that may be associated with the conductive zone are weak and are partially masked by SP effects that result from variations of the depth to the water table associated with wadis or other factors. The SP field is strongly perturbed by the central zone of east-trending structures. However, a pattern of SP anomalies having north-trending axes and amplitudes of from -40 to -70 mV (two to three times background) is associated with the central part of CEM anomalous zone A and probably results from the same sulfide disseminations. The inferred causative body evidently dips too steeply to produce a positive counterpart of the negative belt, and therefore the SP data cannot be used to provide an independent estimate of dip angle (see Telford, 1976). However, the half-width of an SP anomaly is approximately equal to the depth to its source, and, on this basis, inspection of the map and profiles yields source depths of approximately 20 m for the northern part of the negative belt and approximately 10 m for the southern part, where the anomalies narrow. These depths are somewhat less than those estimated from the CEM data.

MAXMIN electromagentic and ground-magnetic surveys

It is now well known that the westernmost part of the Arabian Shield and adjacent coastal plain are the locus of extensive mafic dike intrusion associated with the tectonic evolution of the Red Sea rift and related structures of Tertiary age (Blank, 1977). Several of the larger dikes of this suite in the Al Qunfudhah area were mapped by Hadley (1975), and an aeromagnetic map of the area (unpublished map sheet, scale 1:100,000) suggests that additional mafic intrusive bodies may be present at shallow depths. Therefore small mafic intrusions could be expected to be present in the Umm ar Rummf area, and as noted earlier, several such bodies were mapped by Mawad (unpub. data, 1982).

The first two drill holes in the mineralized zone (UAR-1 and UAR-2, fig. 10) indicate the existence of basaltic intrusive rocks at depth in the vicinity of line 120 N. The MAXMIN electromagnetic and ground-magnetic traverses of lines 80 S, 120 N, and 440 N were carried out to study the effect of basaltic intrusions on the deep conductivity pattern, through direct comparison of the conductivity and magnetic anomalies from deep sources. The profile data from these surveys are shown in figures 11 through 13. MAXMIN profiles 120 N and 80 S (figs. 11 and 12) show weak broad anomalies, which can be attributed to the combined effect of weak conductors in CEM zones A and B and the mafic dike complex. These anomalies are too complex to attempt a quantitative interpretation. Because of equipment malfunction, no MAXMIN data were obtained on traverse line 440 N.

Magnetic profile 120 N (fig. 11) shows a 400-nT, positive magnetic anomaly extending between stations 20 E and 60 W and having a peak at about 30 W. This anomaly coincides with the buried basaltic intrusion intersected by drill hole UAR-1. A similar anomaly, which has a peak at 235 W, was detected on magnetic profile 440 N (fig. 13), and both anomalies approximately coincide with a weak linear aeromagnetic anomaly that strikes N. 30° W., approximately the mean strike of Tertiary dikes along the Red Sea margin. Thus the source of both anomalies is probably a Tertiary mafic dike that is continuous between the two profiles. This dike may or may not be continuous with the transverse dikes mapped by Mawad (1982).

Magnetic profile 80 S (fig. 12) shows only a broad, very weak anomaly, which extends between stations 40 E and 40 W and lacks a sharply defined maximum. The source of this anomaly may be the same intrusion at a greater depth of burial, or it may be a different intrusion having a lower magnetic susceptibility.

The magnetic declination and inclination at Umm ar Rummf are about 1° E. and 24° down, respectively; thus the positive anomaly of an east-trending dike should lie south of its apex. A north-south profile would probably have served much better to delineate these bodies.

CONCLUSIONS

Using data obtained from Crone electromagnetic surveys, two weak north-trending conductors have been mapped in the Umm ar Rummf prospect area. These conductors are interpreted to be sulfide disseminations and fracture fillings at from 20 to 40 m depth along the dip plane (60°-70° E.) of a well-exposed, copper-bearing metaquartzite (western conductor) and

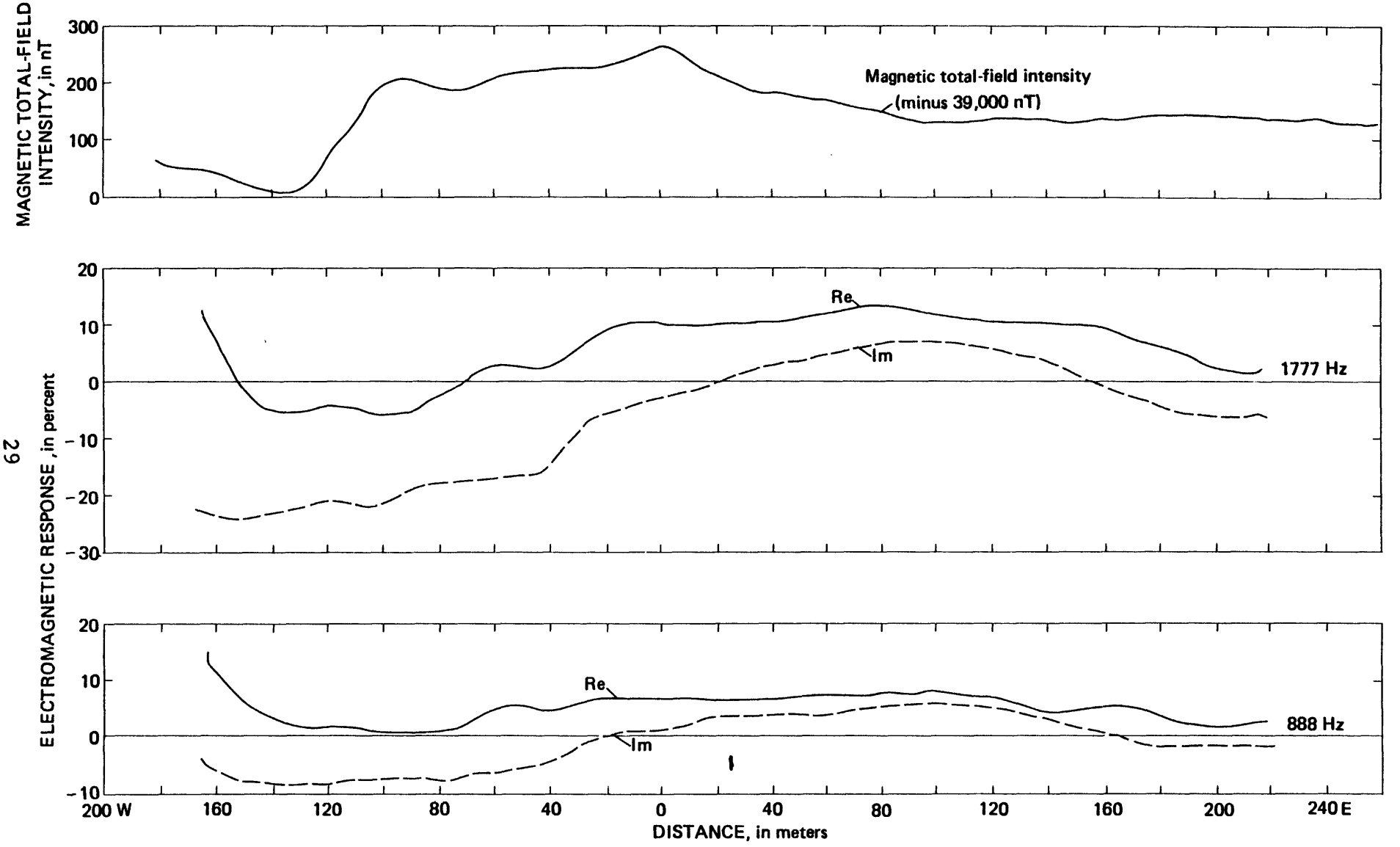

Figure 12.--Profiles showing MAXMIN electromagnetic and ground-magnetic data along line 80 S, Umm ar Rummf prospect. Re = real component; Im = imaginary (quadrature) component of anomalous (secondary) field; Re and Im given in percent of primary field at receiver. Electromagnetic coil spacing is 150 m; data point at center of spread.

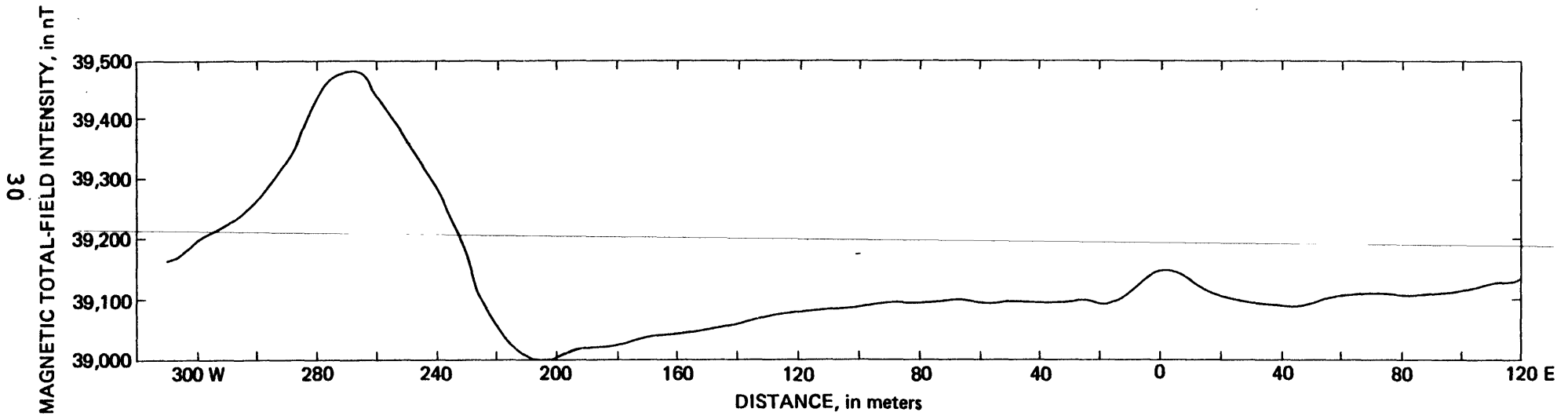

Figure 13.--Profile showing ground-magnetic data along line 440 N,Umm ar Rummf prospect.

a parallel host bed that is mostly concealed (eastern conductor) but probably also metaquartzite. Moreover, the eastern conductor has a considerable extension in a northerly direction along strike at depth and the western conductor has a more limited strike extension at depth to the south. The interpreted depth of burial corresponds roughly to the thickness of the oxidized zone, which constitutes a variably conductive overburden. It is not known if the conductive beds are structural repetitions of a single layer or are stratigraphically discrete. Both conductors are associated with weak, poorly delineated self-potential anomalies having amplitudes of from two to three times background. Groundmagnetic profiles, carried out to delineate the extent of east-trending mafic intrusive rocks that complicate the electrical patterns, have apparently delineated instead a major northwest-trending dike of the Tertiary Red Sea margin set.

It is concluded from this study that Crone electromagnetic surveys are an adequate method for shallow exploration for conductors of this type if the surveys are carried out using the optimum mode and survey parameters for the task. However, because of the disseminated nature of the mineralized rocks and the weak conductivity response, perhaps an induced-polarization exploration method would have served equally well or better to delineate the Umm ar Rummf targets. Deeper penetration could be attempted using mise-a-la-masse techniques or electromagnetic profile surveys having wide coil spacing and adequate power levels.

The proven association of conductor anomalies with copper-mineralized rocks leads us to suggest that further test drilling be carried out to determine the grade of mineralized rocks beneath the most intense Crone electromagnetic/self-potential anomalies in areas where no mineralized rocks crop out. The most intense CEM anomaly was in the southern part of the eastern conductor (zone A, plates 3 and 4), and this anomaly could be tested by a drill hole sited at station 160 E, line 40 S, and having an inclination of 45° W. We recommend an additional drill hole having the same orientation sited at station 160 E, line 400 N; this would test Crone electromagnetic conductors in the northern part of the area. Both holes should extend far enough west to transect the western conductor (zone B, plates 3 and 4).

REFERENCES CITED

Blank, H. R., Jr., 1977, Aeromagnetic and geologic study of Tertiary dikes and related structures on the Arabian margin of the Red Sea, in Red Sea research 1970-1975: Saudi Arabian Directorate General of Mineral Resources Bulletin 22, p. G1-G18.

Crone, J. D., 1966, The development of a new ground EM method for use as a reconnaissance tool, in Mining geophysics, v. 1: Tulsa, Society of Exploration Geophysicists, p. 151-156.

Earhart, R. L., 1969, Geologic reconnaissance of the Al Qunfudhah area, Tihamat Ash Sham quadrangle, Kingdom of Saudi Arabia: U.S. Geological Survey Open-File Report (IR)SA-97, 46 p.

Flanigan, V. J., 1970, Geophysical reconnaissance of sites in the Precambrian Shield, Kingdom of Saudi Arabia--Pt. 1, Evaluation of an electromagnetic anomaly in the Suk al Khamis area; Pt. 2, Electromagnetic reconnaissance of the Wadi Fig and Mahawiyah areas: U.S. Geological Survey Open-File Report (IR)SA-115, 15 p.

Greenwood, W. R., Roberts, R. J., and Bagdady, A. Y., 1974, Mineral belts in western Saudi Arabia: Arab Conference Mineral Resources, 2nd Jiddah, Saudi Arabia, 1974, Conf. Doc. Background papers, Misc. p. 130-151.

Hadley, D. G., 1975, Geology of the Al Qunfudhah quadrangle, sheet 19/41 C, Kingdom of Saudi Arabia: Saudi Arabian Directorate General of Mineral Resources Map GM-19, 11 p., scale 1:100,000.

Lin, Wunan, 1969, A model study of the Crone shootback EM method: Ph.D thesis, University of California, College of Engineering, 37 p.

Schmidt, D. L., Hadley, D. G., Greenwood, W. R., Gonzalez, Louis, Coleman, R. G., and Brown, G. F., 1973, Stratigraphy and tectonism of the southern part of the Precambrian Shield of Saudi Arabia: Saudi Arabian Directorate General of Mineral Resources Bulletin 8, 13 p.

Telford, W. M., Geldart, L. P., Sheriff, R. E., and Keys, D. A., 1976, Applied geophysics: New York, Cambridge University Press, 860 p.